



CHORUS

This is the accepted manuscript made available via CHORUS. The article has been published as:

Surface Energy as a Barrier to Creasing of Elastomer Films: An Elastic Analogy to Classical Nucleation

Dayong Chen, Shengqiang Cai, Zhigang Suo, and Ryan C. Hayward

Phys. Rev. Lett. **109**, 038001 — Published 16 July 2012

DOI: [10.1103/PhysRevLett.109.038001](https://doi.org/10.1103/PhysRevLett.109.038001)

**Surface energy as a barrier to creasing of elastomer films:
An elastic analogy to classical nucleation**

Dayong Chen,¹ Shengqiang Cai,² Zhigang Suo,^{2,*} Ryan C. Hayward^{1,*}

¹Department of Polymer Science & Engineering, University of Massachusetts, Amherst, MA
01003

²School of Engineering and Applied Sciences, Harvard University, Cambridge, MA

*e-mail: suo@seas.harvard.edu, rhayward@mail.pse.umass.edu

Abstract

In a soft elastic film compressed on a stiff substrate, creases nucleate at preexisting defects, and grow across the surface of the film like channels. Both nucleation and growth are resisted by the surface energy, which we demonstrate by studying creases for elastomers immersed in several environments—air, water and an aqueous surfactant solution. Measurement of the position where crease channeling is arrested on a gradient thickness film provides a uniquely characterized strain that quantitatively reveals the influence of surface energy, unlike the strain for nucleation, which is highly variable due to the sensitivity to defects. We find that these experiment data agree well with the prediction of a scaling analysis.

When a soft elastic solid—a gel or an elastomer—is compressed beyond a critical strain, the free surface suddenly forms creases, singular regions of self-contact. This instability has been implicated in the failure of photographic films [1], rubber tires [2], dielectric elastomer actuators [3], and biomedical gel coatings [4]. Creases have also been exploited in devices for reversible sequestration of biomolecules [5] and tunable adhesion [6], and to form dynamic patterns on curved surfaces [7].

While creases are ubiquitous in nature and engineering, a physical understanding has emerged only recently that creases represent a fundamentally distinct type of instability from wrinkles [8-11]. Both are bifurcations from a state of homogenous compression. However, wrinkles bifurcate from the homogenous state by a field of strain small in amplitude and nonlocal in space, while creases bifurcate by a field of strain large in amplitude and localized in space. Although wrinkles of a compressed free surface are predicted theoretically [12], they are preceded by creases, which form at lower compression [2]. Unlike wrinkles, which form by a linear perturbation, creases form by nucleation and growth [13,14]. The origin of this latter behavior, however, has remained unclear, as elasticity predicts a transition from the flat to creased states with no barrier [8-10].

We show here that nucleation and growth of creases can be understood in close analogy to classical nucleation theory for a thermodynamic phase transition [15]. When the compression is high, forming a crease reduces elastic energy by an amount that scales with the deformed volume. However, it also increases the surface area, and thus for an incipient crease, surface energy provides a nucleation barrier. This behavior is also reminiscent of the formation of cracks [16], dislocations [17] and cavities [18], phenomena that are of great technological significance, and present scientific challenges concerning nucleation. While surface energy has been hypothesized to play a role in formation of creases and wrinkles [13,19], past work has

focused on swelling of hydrogels where the surface energy is small and difficult to measure, thus quantitative verification has not been possible.

We study nucleation and growth of creases by compressing a soft elastomeric film on a stiff substrate, and by varying the surface energy using different environments. Creases nucleate at preexisting defects, and then grow—or channel—across the surface of the film. Due to the defect sensitivity, the strain for heterogeneous nucleation is not uniquely characterized, but the strain for channeling is. We design an experiment in which channeling creases arrest in a film of gradient thickness, and find that measured channeling strains agree well with the predictions of a scaling analysis. The importance of surface energy is further demonstrated by the propensity of creases to leave behind long-lived scars stabilized by surface self-adhesion upon unloading of the material.

Our experiments involve two bonded elastomer layers (Fig. 1). We pre-stretch a thick, stiff substrate of polydimethylsiloxane (PDMS) to length L , and then attach a thin unstressed layer of softer PDMS. The shear moduli of the substrate and the film are 270 and 16 kPa, respectively, while the undeformed thickness of the film H varies from 8 to 30 μm depending on spin coating speed. When the substrate is partially released to length l , the film is compressed to a strain of $\varepsilon = (L - l)/L$, but the interface between the film and substrate remains bonded and nearly planar [14].

The surface energy γ is varied by conducting experiment in three environments: air, water, and an aqueous solution of the surfactant 3-[hydro(polyethyleneoxy)propyl]heptamethyltrisiloxane (Gelest) above its critical micelle concentration. Values of γ are 21, 40 and 0.8 mN/m, respectively, as measured by pendent drop tensiometry on uncured PDMS (Sylgard 184 base, Dow Corning) in contact with the corresponding fluid; those for PDMS/air and PDMS/water agree with literature values [20].

The surface energy and shear modulus μ of the film together define a material-specific length γ/μ , which is fundamental to many elastocapillary phenomena [21-23] and is closely related to the elasto-adhesive length involved in contact [24] and fracture mechanics [16]. In our experiments γ/μ varies from ~ 50 nm for the PDMS/surfactant interface to ~ 2.5 μm for PDMS/water.

The bilayer setup allows us to vary the strain in the film, and observe in situ the nucleation and growth of creases in an optical microscope. For example, consider a film, thickness $H = 25$ μm , compressed in the surfactant solution (Fig. 1). Compression is applied quasi-statically, with each increment in strain (~ 0.01) followed by 30 min prior to the next increment. The creases nucleate at preexisting defects, and then channel across the surface of the film. The behavior of the creases bears remarkable resemblance to channeling cracks [25] and threading dislocations [26] in thin solid films. At larger strains, additional creases nucleate and grow, leading to a quasi-periodic array of parallel creases with spacing proportional to H . In Fig. 1, creases first grow across the surface of the film at a strain of $\varepsilon = 0.488$, well above the critical strain of $\varepsilon_0 = 0.438$ in the absence of surface energy [10,14]. As we show below, this over-strain behavior is closely analogous to the supercooling of a clean liquid well below its melting point in that both phenomena are caused by the energy barrier due to surface energy.

Preexisting defects serve as heterogeneous nucleation sites for creases, preventing identification of a unique critical strain for nucleation. To quantitatively test the effects of surface energy, we thus design an experiment in which channeling creases arrest in a film of gradient thickness (Fig. 2). The films are made by spin-coating uncured PDMS on a glass slide, placing the PDMS film on the pre-stretched substrate, and then curing, providing a variation in thickness from 10 μm at the edge to 0.5 μm in the center. When the film is compressed, creases nucleate at the thick edge of the film, and channel toward the center. For a fixed applied strain, the creases arrest in the film at a position where the thickness becomes sufficiently small.

Measuring the thickness of the film at the front where channeling is arrested as a function of applied strain then provides a quantitative measure of the influence of surface energy, where the nature of the nuclei becomes irrelevant. The only geometric length is the thickness of the film, thus the system is characterized by a single dimensionless elastocapillary number $\gamma/(\mu H)$ that governs the strain required for channeling $\varepsilon_{channel}$ (Fig. 2b). Motivated by the scaling analysis below, we fit the measured over-strain to a power law, $\varepsilon_{channel} - \varepsilon_o = \alpha(\gamma/\mu H)^\beta$, with $\alpha = 0.17 \pm 0.01$ and $\beta = 0.49 \pm 0.06$.

An additional experiment demonstrates that surface energy resists both nucleation and channeling of creases. A film of gradient thickness is compressed in water to a strain of $\varepsilon = 0.513$, causing creases nucleated at the sample edge to channel a certain distance and then arrest. Without changing the strain, the surface is flooded with surfactant solution, lowering γ by 50-fold. This causes arrested creases to resume channeling into the thinner region of the film, and also leads to nucleation of new creases in the thinner regions of the sample (Video 1). As creases channel from the thick to the thin regions of the film, the formation of additional creases is required to maintain the minimum-energy spacing of $W/H \approx 3.5$ [14], yielding a hierarchical cascade of creases (Fig. S1).

We next perform a scaling analysis following Yoon, et al. [13], but with coefficients determined by finite-element calculation (described in the Supplementary Information). In a state of equilibrium, let a be the length of the self-contacting region along the direction of the film thickness, and ΔU be the difference in energy per unit length of crease between the creased state and the homogeneously compressed state. We treat ΔU as the sum of two independent terms representing the surface energy ΔU_s and the elastic energy ΔU_e . For a shallow crease, $a \ll H$, the length of contact a is the only geometric length in the boundary value problem. That is, a crease is always of aspect ratio near one, with its lateral dimensions and depth both

scaled with a , and therefore dimensional considerations give that $\Delta U_s \propto \gamma a$. We fit the calculated surface energy to the expression $\Delta U_s = A\gamma a$, with $A = 0.45$ (Fig. S2).

We next consider the elastic energy due to the formation of a crease. For a shallow crease, $a \ll H$, dimensional considerations dictate that the excess elastic energy scales as $\Delta U_e = \mu a^2 f(\epsilon)$, where $f(\epsilon)$ is a dimensionless function [10]. In the absence of surface energy, a crease may form at the critical strain of $\epsilon_0 = 0.438$. That is, $f(\epsilon_0) = 0$ and $f(\epsilon) > 0$ when $\epsilon < \epsilon_0$. Near ϵ_0 , the function $f(\epsilon)$ can be taken as linear in the over-strain, so that $\Delta U_e \approx -B\mu(\epsilon - \epsilon_0)a^2$, where B is a positive constant. However, when the size of the crease a is a significant fraction of the thickness of the film H , deepening of the crease is repelled by the rigidity of the substrate, which we capture through a third-order term in a : $\Delta U_e \approx -B\mu(\epsilon - \epsilon_0)a^2 + C(\mu/H)a^3$, where C is a positive constant [13]. We neglect terms of higher orders of a , and assume that $|\epsilon - \epsilon_0|$ is small, such that B and C are calculated at $\epsilon = \epsilon_0$. Fitting this expression to the calculated elastic energy (Fig. S2), we obtain $B = 13.5$ and $C = 2.4$.

For an incipient crease much smaller than the thickness of the film, surface energy provides a barrier to the nucleation of a crease, but the effect of the substrate is negligible. The excess energy is then $\Delta U(a) \approx A\gamma a - B\mu(\epsilon - \epsilon_0)a^2$, yielding a dependence on length analogous to that in classical nucleation theory (Fig. 3). The term due to surface energy resists formation of the crease, while the term due to elasticity motivates formation of the crease for $\epsilon > \epsilon_0$. For nuclei below the critical size, surface energy prevails, and the total energy is reduced when the nucleus shrinks. Above the critical size, elastic energy prevails, and the total energy decreases when the nucleus grows. Setting $\partial\Delta U(a)/\partial a = 0$, we obtain

$$a_{nuc} \approx \frac{A\gamma}{2B\mu(\epsilon - \epsilon_0)}, \quad (1)$$

or $a_{nuc} = 0.017\gamma/[\mu(\varepsilon - \varepsilon_0)]$ using A and B from the finite-element calculations. For example, considering the film immersed in surfactant solution with an over-strain of $\varepsilon - \varepsilon_0 = 0.05$ (Fig. 1b), the predicted critical nucleus is of size $a_{nuc} = 17$ nm. However, a sizable energetic barrier to creasing remains; in this case about $12 k_B T$ for a critical nucleus whose length is also a_{nuc} . Consequently, creases nucleate heterogeneously at defects, which are present with a distribution of sizes, shapes, and locations in the material, making it difficult to confirm the prediction of Eq. (1). We note that measuring critical nuclei in many thermodynamic phase transitions is a long-standing challenge [15].

By contrast, the effect of surface energy on channeling is well characterized. The condition for channeling creases to arrest in a film of gradient thickness is independent of preexisting defects, and is determined by the smallest thickness where the energy curve touches zero for a finite crease depth, i.e. when $\partial\Delta U/\partial a = 0$ and $\Delta U = 0$ (represented in Fig 3 by the curve at $\varepsilon = 0.460$). Writing the excess energy as $\Delta U = A\gamma a - B\mu(\varepsilon - \varepsilon_0)a^2 + C(\mu/H)a^3$, we obtain the over-strain for channeling:

$$\varepsilon_{channel} - \varepsilon_0 = \frac{2\sqrt{AC}}{B} \left(\frac{\gamma}{\mu H} \right)^{1/2}, \quad (2)$$

or $\varepsilon_{channel} - \varepsilon_0 = 0.15(\gamma/\mu H)^{1/2}$ using A , B and C from the finite-element calculations. The theoretically predicted pre-factor and the exponent agree well with those determined from the experimental data, as also seen from the comparison in Fig. 2b.

For the largest value of the elastocapillary number considered, $\gamma/(\mu H) = 0.86$, the measured channeling strain is $\varepsilon_{channel} = 0.60$, far above the critical strain in the absence of surface energy, $\varepsilon_0 = 0.438$, and even above Biot's prediction of linear instability for wrinkling of the compressed surface, $\varepsilon_{Biot} = 0.56$ [12]. This raises the question of whether surface energy can suppress creasing to the point that the surface becomes linearly unstable first. However, as described in the Supplementary Information and summarized in the inset to Fig. 2, when

surface energy is included in the perturbation analysis for elastomer films, as studied previously by Huang and co-workers for gels [19], linear instability is suppressed even more. Thus, while a large value of $\gamma/(\mu H)$ delays the onset of creasing to greater strains, it should not provide a qualitative change in the mechanism of instability.

We finally turn to the hysteresis observed during loading, unloading and reloading of elastomer films. In most experimental systems studied [2,8,28-30] (with the notable exception of hydrogels with relatively low polymer concentration [5,13,27]), creases leave permanent “scars”, allowing them to re-form at lower strains in the second and subsequent loading cycles. We observe similar behavior for PDMS films compressed in air (Fig 4a). During the first loading, a strain of $\varepsilon = 0.520$ is required for creases to nucleate and channel, and this over-strain leads to a discontinuous jump from a smooth surface to creases of finite depth, as indicated by the solid black line. The depth of the creases (as estimated by optical profilometry of the free surface) decreases smoothly towards zero upon unloading, but scars remain even at $\varepsilon = 0$. While these features diminish in amplitude somewhat over time, they remain visible after several days (Fig. 4b). During the second loading, scars become creases (as judged by the change in slope of depth versus strain) at a lower strain than that required for the nucleation of the creases during the first loading (Video 2). Indeed, the scar-to-crease transition occurs at a strain comparable to the channeling strain.

One might expect that this behavior reflects plastic deformation or material failure at the singular crease tip, thus leading to weak spots that facilitate crease initiation during subsequent cycles. However, strikingly different behavior is found for films compressed in the surfactant solution (Video 3). In this case, scars are observed when compression is removed, but they completely disappear within 12 h of unloading. Reloading then leads to nucleation and growth of creases in essentially identical fashion as during the first cycle, showing that scars are not due to plastic deformation, but instead arise from adhesion in the regions of self-contact. As a crease is peeled apart during unloading, the elastic driving force per unit length diminishes

linearly with crease depth d . For a surface with significant self-adhesion, this force will ultimately fall below the critical strain energy release rate G_c to propagate the “crack” between the self-contacting surface, thus leading to a finite steady-state scar depth $d_s \sim G_c / \mu$.

In summary, surface energy provides a barrier to nucleation of creases and also resists their channeling for finite values of the elastocapillary number. While heterogeneous nucleation complicates characterization of the critical strain for nucleation, the condition for channeling is well characterized and depends on the elastocapillary number. Adhesion, rather than plastic deformation, is responsible for the dramatic hysteresis between the first and subsequent cycles of compression.

The work at the University of Massachusetts is supported by the National Science Foundation through grant DMR-0747756. The work at Harvard is supported by MRSEC.

References

- [1] S. E. Sheppard and F. A. Elliott, *Ind. Eng. Chem.*, 10, 727 (1918).
- [2] A. N. Gent and I. S. Cho, *Rubber Chem. Technol.*, 72, 253 (1999).
- [3] Q. Wang, L. Zhang and X. Zhao, *Phys. Rev. Lett.*, 106, 118301 (2011).
- [4] K. Saha, J. Kim, E. Irwin, J. Yoon, F. Momin, V. Trujillo, D. V. Schaffer, K. E. Healy and R. C. Hayward, *Biophysical Journal*, 99, 94 (2010).
- [5] J. Kim, J. Yoon and R. C. Hayward, *Nat. Mater.*, 9, 159 (2010).
- [6] E. P. Chan, J. M. Karp and R. S. Langer, *J of Poly. Sci.: Part B: Polymer Phys.*, 49, 40 (2011).
- [7] Q. Wang, M. Tahir, J. Zang and X. Zhao, *Adv. Mater.*, 24, 1947 (2012).
- [8] E. B. Hohlfeld, PhD thesis, Harvard University (2008).
- [9] E. Hohlfeld and L. Mahadevan, *Phys. Rev. Lett.*, 106, 105702 (2011).
- [10] W. Hong, X. Zhao and Z. Suo, *Appl. Phys. Lett.*, 95, 111901 (2009).
- [11] Y. Cao, J.W. Hutchinson, *Proc. R. Soc. A*, 468, 94 (2012).
- [12] M. A. Biot, *Appl. Sci. Res., Sect. A*, 12, 168 (1963).
- [13] J. Yoon, J. Kim and R. C. Hayward, *Soft Matter*, 6, 5807 (2010).
- [14] S. Cai, D. Chen, Z. Suo, R. C. Hayward, *Soft Matter*, 8, 1301 (2012).
- [15] K. F. Kelton and A. L. Greer, *Nucleation in Condensed Matter*, Elsevier (2010).
- [16] A. A. Griffith, *Philosophical transactions of the Royal society of London*, 221, 163 (1921).
- [17] L. B. Freund, *J. Mech. Phys. Solids*, 38, 657 (1990).
- [18] A. N. Gent, *Rubber Chem. Tech.*, 63, G49 (1991).
- [19] M. K. Kang and R. Huang, *Soft Matter*, 6, 5736 (2010).
- [20] M. K. Chaudhury and G. M. Whitesides, *Langmuir*, 7, 1013 (1991).
- [21] J. Bico, B. Roman, L. Moulin and A. Boudaoud, *Nature*, 432, 690 (2004).
- [22] J. Huang, M. Juskiewicz, W. H. de Jeu, E. Cerda, T. Emrick, N. Menon and T. P. Russell, *Science*, 317,650 (2007).
- [23] T. Jamin, C. Py, and E. Falcon, *Phys. Rev. Lett.*, 107, 20450 (2011).
- [24] K. L. Johnson, K. Kendall and A. D. Roberts, *Proc. R. Soc. A*, 324, 301 (1971).
- [25] K. W. McElhane and Q. Ma, *Acta Mat.*, 52, 3621 (2004).
- [26] C. W. Leitz, M. T. Currie, A. Y. Kim, J. Lai, E. Robins and E. A. Fitzgerald, *J. Appl. Phys.*, 90, 2730 (2001).
- [27] T. Tanaka, S. T. Sun, Y. Hirokawa, S. Katayama, J. Kucera, Y. Hirose and T. Amiya, *Nature*, 325, 796 (1987).

- [28] M. Guvendiren, S. Yang and J. A. Burdick, *Adv. Funct. Mater.*, 19, 3038 (2009).
- [29] O. Ortiz, A. Vidyasagar, J. Wang and R. Toomey, *Langmuir*, 26, 17489 (2010).
- [30] A. Ghatak and A. L. Das, *Phys. Rev. Lett.*, 99, 076101 (2007).

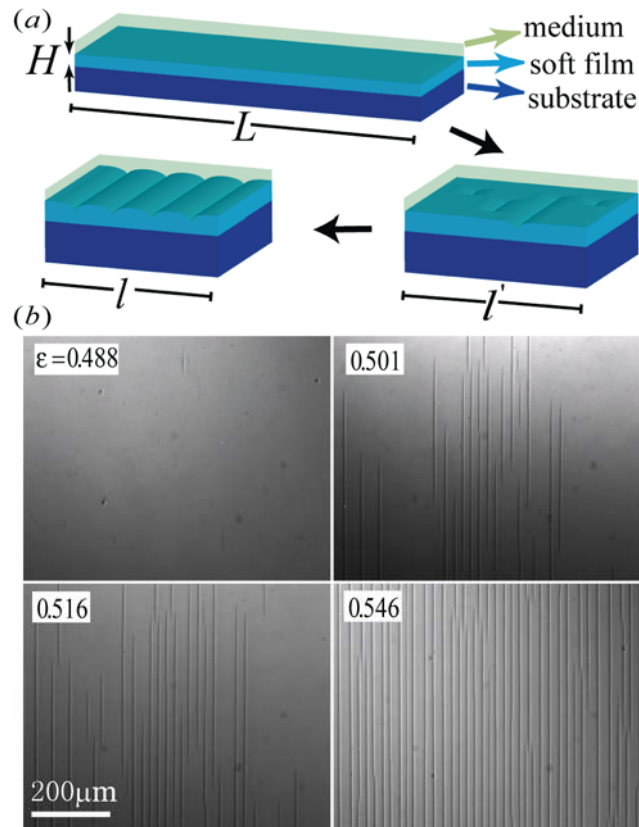


FIG. 1 (color online). An experiment to study nucleation and growth of creases. (a) A thick substrate of stiff elastomer is stretched to L , then a stress-free film of soft elastomer, thickness H , is attached. The bilayer is submerged in a medium to define the surface energy. When the substrate is partially released to l' , the film is compressed, and creases nucleate. When the substrate is further released to l , creases channel across the surface. (b) Nucleation and growth of creases as observed by reflection optical microscopy. The strain in the film is defined as $\varepsilon = (L-l)/L$.

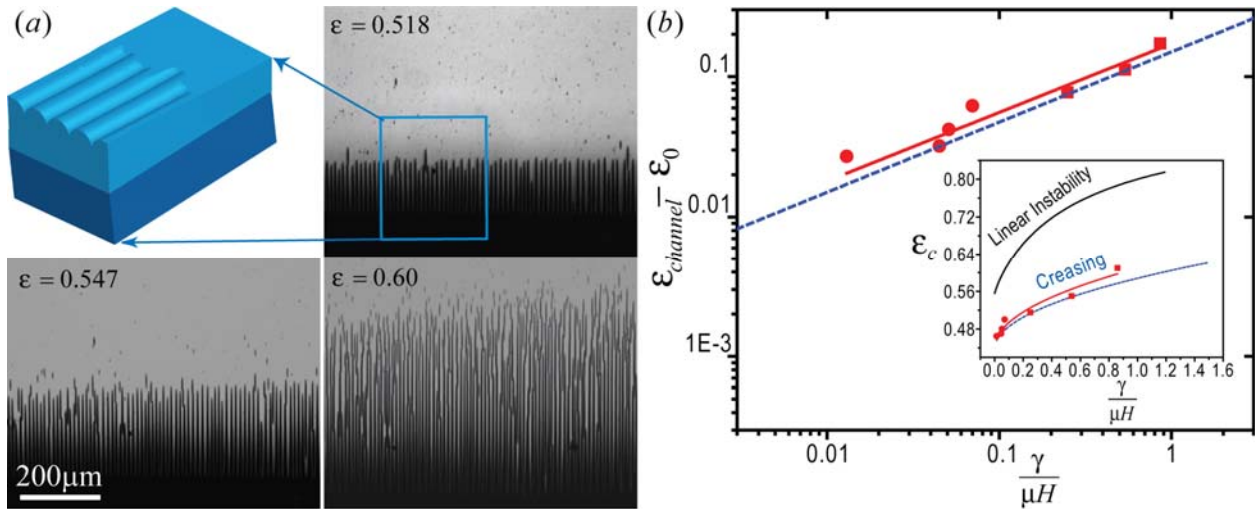


FIG.2 (color online). A comparison of experiments and predictions for crease channeling. (a) An illustration and reflection optical micrographs of creases channeling from thick to thin regions in a gradient thickness film, in contact with air. (b) The overstrain required for channeling is plotted against the dimensionless elasto-capillary number. Filled symbols are experimental results for contact with surfactant solution (circles) and air (squares), with uncertainties smaller than the markers. The solid line represents the best-fit power law, while the dotted line is the theoretical prediction.

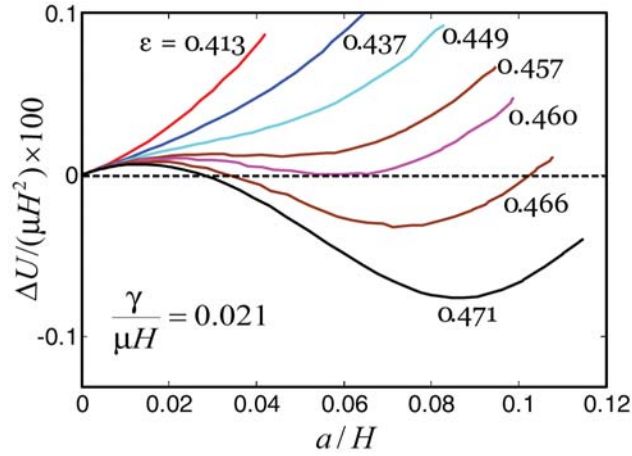


FIG.3 (color online). The combined elastic and surface energies in the creased state, relative to the homogeneously compressed state, plotted against the normalized length of surface contact. Calculated curves are shown at different levels of the applied strain for a single value of the elasto-capillary number.

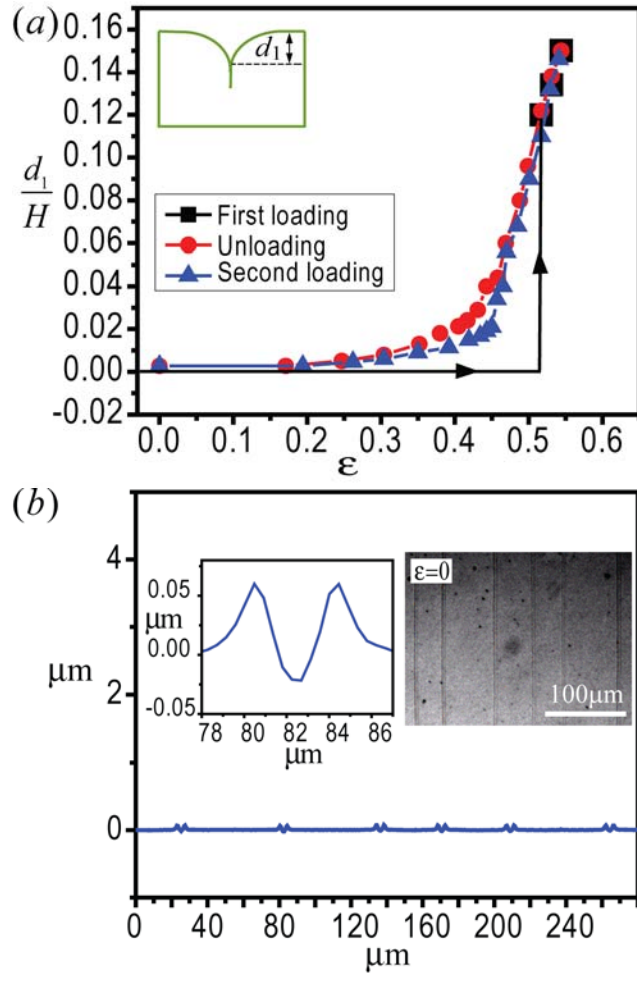


FIG. 4 (color online). (a) The depth of a crease for a PDMS/air interface shows large hysteresis between the first loading and subsequent unloading/reloading cycles due to formation of adhesion scars. (b) An optical surface profile shows that scars remain even after the complete removal of compression. The right inset shows a top view optical micrograph of the surface, while the left inset highlights a single scar.